Atmospheric Environment 44 (2010) 2767–2779

Contents lists available at ScienceDirect

Atmospheric Environment

journal homepage: www.elsevier.com/locate/atmosenv

Responses of future air quality to emission controls over North Carolina, Part II: Analyses of future-year predictions and their policy implications

Yang Zhang [a,*], Xiao-Huan Liu [a,b], Kristen M. Olsen [a], Wen-Xing Wang [b], Bebhinn A. Do [c], George M. Bridgers [c]

[a] Department of Marine, Earth, and Atmospheric Sciences, North Carolina State University, Raleigh, NC 27695, USA
[b] Environment Research Institute, Shandong University, 27 Shanda Nanlu, Jinan, Shandong Province, PR China 250100
[c] Division of Air Quality, North Carolina Department of Environment and Natural Resources, Raleigh, NC 27699, USA

ARTICLE INFO

Article history:
Received 2 December 2009
Received in revised form
17 March 2010
Accepted 17 March 2010

Keywords:
MM5/CMAQ
Impact of emissions on future air quality
Air quality standard attainment
Sensitivity to horizontal grid resolution

ABSTRACT

The MM5/CMAQ system evaluated in Part I paper is applied to study the impact of emission control on future air quality over North Carolina (NC). Simulations are conducted at a 4-km horizontal grid resolution for four one-month periods, i.e., January, June, July, and August 2009 and 2018. Simulated $PM_{2.5}$ in 2009 and 2018 show distribution patterns similar to those in 2002. $PM_{2.5}$ concentrations over the whole domain in January and July reduced by 5.8% and 23.3% in 2009 and 12.0% and 35.6% in 2018, respectively, indicating that the planned emission control strategy has noticeable effects on $PM_{2.5}$ reduction in this region, particularly in summer. More than 10% and 20% of 1-h and 8-h O_3 mixing ratios are reduced in July 2009 and 2018, respectively, demonstrating the effectiveness of emission control for O_3 reduction in summer. However, O_3 mixing ratios in January 2009 and 2018 increase by more than 5% because O_3 chemistry is VOC-limited in winter and the effect of NO_x reduction dominates over that of VOC reduction under such a condition. The projected emission control simulated at 4-km will reduce the number of sites in non-attainment for max 8-h O_3 from 49 to 23 in 2009 and to 1 in 2018 and for 24-h average $PM_{2.5}$ from 1 to 0 in 2009 and 2018 based on the latest 2008 O_3 and 2006 $PM_{2.5}$ standards. The variability in model predictions at different grid resolutions contributes to 1–3.8 ppb and 1–7.9 μg m^{-3} differences in the projected future-year design values for max 8-h O_3 and 24-h average $PM_{2.5}$, respectively.

1. Introduction

Air quality attainment for future-years posts significant challenges in emission control technologies, regulation revision and enforcement, as well as decision tool development and application. CMAQ is one of the decision tools for regulatory applications developed by the U.S. EPA. Several global and regional models including MM5/CMAQ have recently been applied to simulate future air quality and their responses to future climate changes and/or emission changes either as a result of changing climate (e.g., biogenic emissions) or as part of the emission control programs (e.g., anthropogenic emissions) (e.g., Hogrefe et al., 2004; Liao et al., 2006; Arunachalam et al., 2006; Tagaris et al., 2007; Wu et al., 2008a; Zhang et al., 2008). Most of these studies are conducted at a regional scale (≥36-km) and focus only on surface ozone (O_3). Very few focus on fine particulate matter ($PM_{2.5}$) and consider the changes in biogenic and/or anthropogenic emissions (e.g., Tagaris et al., 2007; Zhang et al., 2008). Since O_3 and $PM_{2.5}$ share common emission sources and precursors, studies excluding each other may not provide a complete description of future air quality and an emission control strategy focusing on one pollutant may not lead to an overall improvement of future air quality. For example, a reduction in emissions of volatile organic compounds (VOCs) may decrease O_3 but increase particulate nitrate formation (Meng et al., 1997; Liu et al., in press a). The effectiveness of the emission control strategies depends on chemical and meteorological conditions due to the complex, non-linear interplays of chemical and meteorological processes during the formation of O_3 and $PM_{2.5}$. For example, O_3 can be most effectively reduced by reducing NO_x under the NO_x-limited conditions or by reducing VOCs under the VOC-limited conditions. Tsimpidi et al. (2007) found that NH_3 emission control during winter time is a more effective and less costly control strategy than reducing NO_x and SO_2 emissions. Emission control strategies therefore require a careful design to reflect the characteristics of emissions, chemistry, and meteorology of regions of interest. In this Part II paper, the impact of emission control on

* Corresponding author. Tel.: +1 919 515 9688; fax: +1 919 515 7802.
E-mail address: yang_zhang@ncsu.edu (Y. Zhang).

1352-2310/$ – see front matter
doi:10.1016/j.atmosenv.2010.03.022

future air quality will be evaluated by using CMAQ v4.5.1 described and evaluated in Part I (Liu et al., in press b). The effectiveness of the projected emission controls under winter and summer conditions will be assessed. As shown in Part I, the performance of MM5/CMAQ for January and July 2002 simulations is overall consistent with that reported in the literature, although some large biases occur for temperature at 1.5 m in January, precipitation in both months, and 24-h average $PM_{2.5}$ concentrations in July. Compared with the simulation at 12-km, the 4-km simulation gives slightly larger biases for maximum 1-h and 8-h average mixing ratios of O_3, 24-h average concentrations of $PM_{2.5}$ and most $PM_{2.5}$ components, and visibility parameters, but lower biases for EC and OM in January and wet deposition fluxes of NH_4^+ and NO_3^- in July.

The state implementation plan (SIPs) modeling for multiple pollutants is expected to be conducted at a grid resolution of 12-km or finer (U.S. EPA, 2007). Several studies have evaluated the sensitivity of model predictions over NC to horizontal grid resolution. For example, Arunachalam et al. (2006) evaluated the impact of grid resolution on O_3 simulated by the Multiscale Air Quality Simulation Platform (MAQSIP) for 19–25 June 1996 and a few days in summers 1995–1997, respectively. Neither work assessed the impacts of grid resolution on meteorology, $PM_{2.5}$, visibility, and dry and wet deposition amounts, some of these were examined in Wu et al. (2008b) and Queen and Zhang (2008) at 4-, 12-, and 36-km for both August and December 2002 using CMAQ and an older version of the VISTAS's emissions, and all of these have been examined at 4- and 12-km for both January and July 2002 using a variant of CMAQ and the latest VISTAS's emissions in Liu et al. (in press b). Evaluation of such impacts has not been done for future-year simulations and for a complete set of model outputs over NC, which is another focus of this Part II paper. Such an evaluation aims to address some policy-related concerns regarding whether the model results at 4-km significantly differ from those at 12-km in terms of temporal variation, spatial distribution, and performance statistics and what species exhibit a large sensitivity; what the policy implications of such a sensitivity are to the SIP modeling; and what additional information can fine-scale simulations provide for SIP and future design values for O_3 and $PM_{2.5}$.

2. Responses of air quality to emission reductions in 2009 and 2018

Fig. 1 shows the emissions of major pollutants in current and future years and corresponding domain-average percentage reductions from the level of 2002–2009 and 2018 for these emissions and concentrations of O_3 and $PM_{2.5}$. CO, an important O_3 precursor under rural conditions, is mainly emitted from motor vehicles in NC, with a total of 4,164,158 tons in 2002 and projected 19.7% and 32.6% reductions in 2009 and 2018, respectively, from the 2002 level. NO_x, an important precursor of O_3 and PM nitrate, is predominantly from Electric Generating Units (EGUs) and traffic sources. A total of 643,448 tons of NO_x are emitted in 2002, with projected 35.4% and 56.5% reductions in 2009 and 2018, respectively. In contrast to emission reductions in NO_x, CO, SO_2, and VOCs, the emissions of NH_3 and $PM_{2.5}$ increase by up to 14.1% and 16.4% in 2018, respectively. NC ranks the second among all U.S. states in terms of hog production (Wu et al., 2008b), with a total of 173,185 tons of NH_3 emitted from NC and 6.5% and 14.1% increase in 2009 and 2018 respectively, due to projected potential increases in hog productions in the eastern NC and potential increases in other sources in the northwest and central NC. In responses to changes in emissions, O_3 mixing ratios increase in January and decrease in June, July, and August; the concentrations of $PM_{2.5}$ and its composition decrease in all the four months, with larger reduction in summer months than in January for all species except for OM. For example, the domain-wide max 1-h and 8-h O_3 mixing ratios decrease by 9.5–11.7% and 8.3–11.4% in 2009, and 16.6–21.7% and 14.8–20.0% in 2018, respectively, in summer months. The domain-wide concentration reductions in summer months are 19.5–23.3% and 31.1–35.5% for $PM_{2.5}$, 18.1–20% and 32.3–35.6% for NH_4^+, 29.2–35.2% and 48.1–54.5% for SO_4^{2-}, 37.2–44.3% and 54.0–62.8% for NO_3^-, and 17.5–81.2% and 27.9–84.8% for EC, and 3.5–4.4% and 5.7–6.7% for OM in 2009 and 2018, respectively. More detailed results along with reasons for these changes are provided below.

Fig. 2 shows the absolute differences in the spatial distribution of 1-h and 8-h O_3 mixing ratios and $PM_{2.5}$ concentrations in January and July between 2009 and 2002 and between 2018 and 2002. As a direct response to reduced precursor emissions and concentrations, the max 1-h and 8-h O_3 mixing ratios in July are reduced by 2–6 ppb (6–18%) in 2009 and 3.6–10.8 ppb (12–30%) in 2018, respectively, over almost the entire domain. Those in January, however, show increased trends throughout the domain, with an increase of 0.6–5 ppb (2–30%) and 0.6–8 ppb (2–80%) for maximum 1-h and 8-h O_3 mixing ratios in 2009 and 2018, respectively. Different responses in O_3 mixing ratios to emission reductions in January and July are caused by different chemistry in these months. A number of indicators such as H_2O_2/HNO_3, $H_2O_2/(O_3 + NO_2)$, $HCHO/NO_2$, $HCHO/NO_y$, NO_y, O_3/NO_x, and O_3/NO_y have been developed to determine whether O_3 concentrations at a given location are most sensitive to VOC or NO_x emissions (Sillman, 1995; Tonnesen and Dennis, 2000; Zhang et al., 2005). For example, the afternoon values of $NO_y \le 20$ ppb, $H_2O_2/HNO_3 \ge 0.2$, $H_2O_2/(O_3 + NO_2) \ge 0.02$, and $HCHO/NO_2 \ge 1$ indicate a NO_x-limited O_3 chemistry and other values above or below these transition values indicate a VOC-limited O_3 chemistry (Sillman, 1995; Tonnesen and Dennis, 2000). Fig. 3 shows the spatial distributions of H_2O_2/HNO_3, $H_2O_2/(O_3 + NO_2)$, and $HCHO/NO_2$ in January and July 2002. The values of H_2O_2/HNO_3 and $H_2O_2/(O_3 + NO_2)$ are larger than 2 and 0.042 throughout the whole domain in July, indicating a NO_x-limited O_3 chemistry; other indicators such as $HCHO/NO_2$, $HCHO/NO_y$, NO_y, O_3/NO_x, and O_3/NO_y also show a NO_x-limited O_3 chemistry in most NC. Several indicators, however, show a VOC-limited O_3 chemistry in January. This is consistent with the finding by Jacob et al. (1995) who reported a seasonal transition from NO_x- to VOC-limited conditions for O_3 production in the eastern U.S. by analyzing measured concentrations of O_3, CO, NO, NO_y, H_2O_2, and HCHO. It is also consistent with the finding of Pinder et al. (2008) that reducing NO_x emissions leads to an increased O_3 in the eastern U.S. in winter because of VOC-limited condition. The VOC-limited chemistry in winter leads to O_3 increase because the emission reduction of NO_x dominates over that of VOC in winter. Although biogenic VOCs emissions are main sources of VOCs in NC and uncontrollable, more reductions in anthropogenic VOC emissions can help compensate the O_3 increase due to the reduction in NO_x emissions in NC in winter as the NAAQS becomes more stringent and VOCs emission control may play an increasingly important role in future O_3 attainment.

The spatial distributions of $PM_{2.5}$ and its components in future years are similar to those in 2002. For example, the highest $PM_{2.5}$ occurs at central and eastern NC and about 1–2 $\mu g\ m^{-3}$ and 2–3.5 $\mu g\ m^{-3}$ $PM_{2.5}$ are reduced in this area in 2009 and 2018, respectively. Although NH_3 emissions increase in 2009 and 2018, NH_4^+ concentrations decrease due to lower concentrations of NO_3^- and SO_4^{2-} for its neutralization. The temporal variation trends of January $PM_{2.5}$ in 2009 and 2018 are similar with 2002, with greater reductions in peak concentrations (Figures not shown). The simulated $PM_{2.5}$ concentrations in July 2009 are in the range of 6–9 $\mu g\ m^{-3}$ in the most of the domain and those in July 2018 are in the same range but are lower than 6 $\mu g\ m^{-3}$ in the mountain and most coastal areas. Similar to 2002, the highest $PM_{2.5}$ occurs along

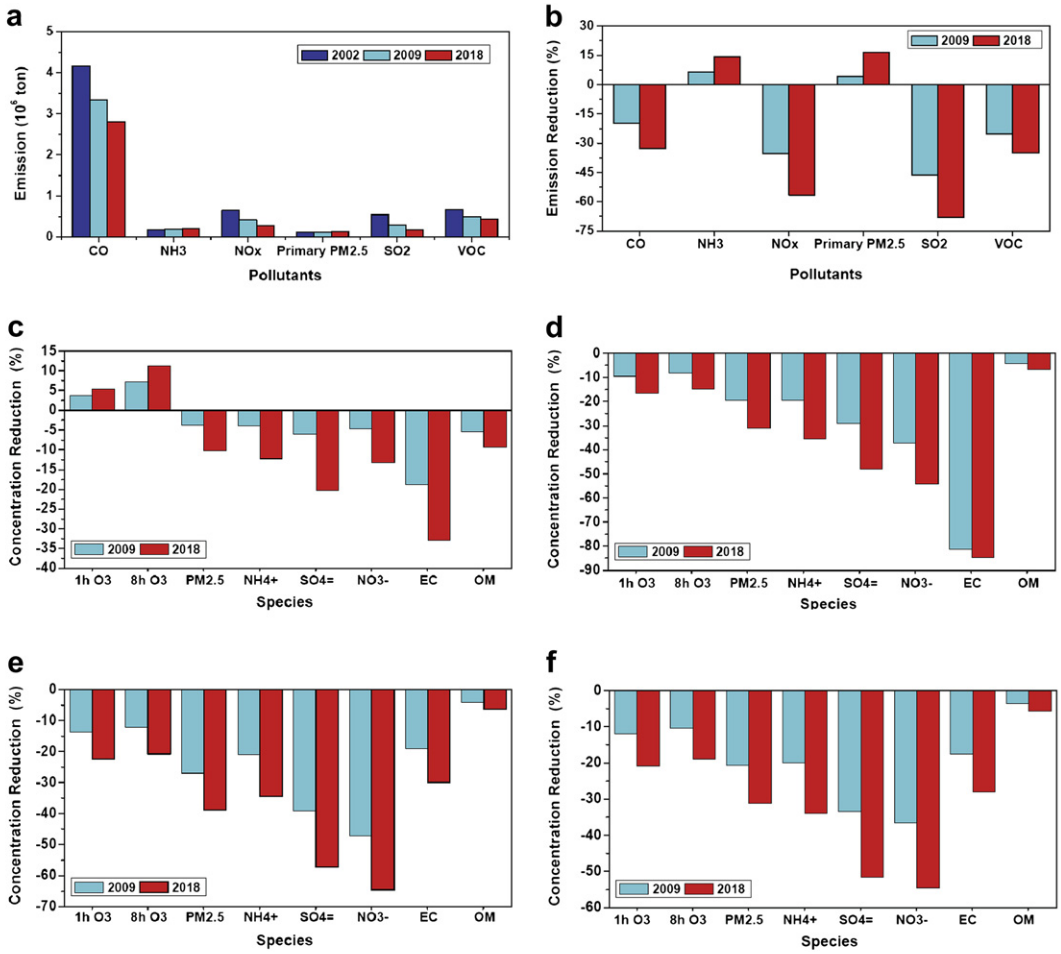

Fig. 1. Emission and chemical species changes at 4-km horizontal grid resolution from 2002 to 2018. (a) Main pollutants emissions in 2002, 2009, and 2018, (b) emission changes in 2009 and 2018, and reduction of chemical species concentrations in 2009 and 2018 in (c) January (d) June (e) July, and (f) August.

the west side of Appalachian Mountains in TN in 2009 and 2018. Compared with July 2002, 24-h average $PM_{2.5}$ concentrations in July 2009 and 2018 are reduced by up to 26.9% and 38.8% for the whole domain (see Fig. 1(c) and (d)), significant reductions occur in the west side of Mountains in KY and TN and in the central NC. The temporal variations of $PM_{2.5}$ in 2009 and 2018 are similar to those in 2002, with significant reductions in peak concentrations (Figures not shown). For SO_4^{2-}, 30% reduction in 2009 and >50% reduction in 2018 occur over nearly entire domain, with >40% reduction in 2009 and ~60% reduction in 2018 in the west side of mountain areas in KY and the central area in NC. For the same reason stated previously, large NH_4^+ concentration decrease (>20% in 2009 and 30% in 2018) occurs in the coastal and central NC, despite an increase in the NH_3 emission in 2009 and 2018. More than 15% and 30% NO_3^- reduction occurs in 2009 and 2018 in most of the domain, with a significant decrease in the coastal area but little or no changes in the mountain areas. The magnitude of reductions in $PM_{2.5}$ is larger in July than in January due to a greater reduction in the concentrations of NH_4^+ and SO_4^{2-} in July, indicating that the planned control strategy is more effective for $PM_{2.5}$ improvement during summer. The areas with high $PM_{2.5}$ concentrations in 2002 are more sensitive to emission reductions in both January and July.

Fig. 4 shows absolute differences in EXT_Recon and DCV_Recon simulated at 4-km between 2009 and 2002 and between 2018 and 2002. In January 2009/2018, the EXT_Recon values are reduced by 6–30 Mm^{-1} (4–10%) and 6–50 Mm^{-1} (6–30%), respectively, and the DCV_Recon values are reduced by 0.2–1.0 dv (2–10%) and 0.4–2.0 dv (4–15%), respectively, over most of domain. Larger reductions occur in July 2009/2018. The EXT_Recon values are reduced by 10–40 Mm^{-1} (10–30%) and 20–60 Mm^{-1} (20–40%), respectively, and the DCV_Recon values are reduced by 0.8–3.2 dv (8–16%) and 2–5 dv (12–24%), respectively, over most of domain. These results indicate an improved visibility in future years because of reduced $PM_{2.5}$ concentrations.

Fig. 5 shows absolute differences in hourly dry deposition amounts of NH_4^+, SO_4^{2-}, and NO_3^- simulated at 4-km between 2009 and 2002 and between 2018 and 2002. The dry deposition amounts are reduced by 2–10 mg ha^{-1} (4–20%) for NH_4^+, 4–20 mg ha^{-1} (14–42%) for SO_4^{2-}, and 6–30 mg ha^{-1} (8–40%) for NO_3^- in January 2009 and 2–20 mg ha^{-1} (8–50%) for NH_4^+, 4–50 mg ha^{-1} (20–60%) for SO_4^{2-}, and 6–50 mg ha^{-1} (8–50%) for NO_3^- in January 2018, respectively, primarily over coastal plain and mountain areas. Some increases in the dry deposition amounts of NO_3^- occur over the west side of Appalachian Mountains and ocean, because of increases in NO_3^- as a result of decreased SO_4^{2-} and availability of more NH_4^+ over the mountain area and availability of Na^+ to neutralize NO_3^- over the ocean. The dry deposition amounts are reduced by 1–5 mg ha^{-1} (8–24%) for NH_4^+, 10–40 mg ha^{-1} (16–48%) for SO_4^{2-}, and 2–10 mg ha^{-1} (16–64%) for NO_3^- in July 2009 and 1–5 mg ha^{-1} (8–40%) for NH_4^+, 10–50 mg ha^{-1} (32–64%) for SO_4^{2-}, and 2–20 mg ha^{-1} (16–80%) for NO_3^- in July 2018, respectively, primarily over coastal plain and Piedmont areas.

Fig. 6 shows absolute differences in the hourly wet deposition amounts of NH_4^+, SO_4^{2-}, and NO_3^- simulated at 4-km between 2009 and 2002 and between 2018 and 2002. In January 2009 and 2018,

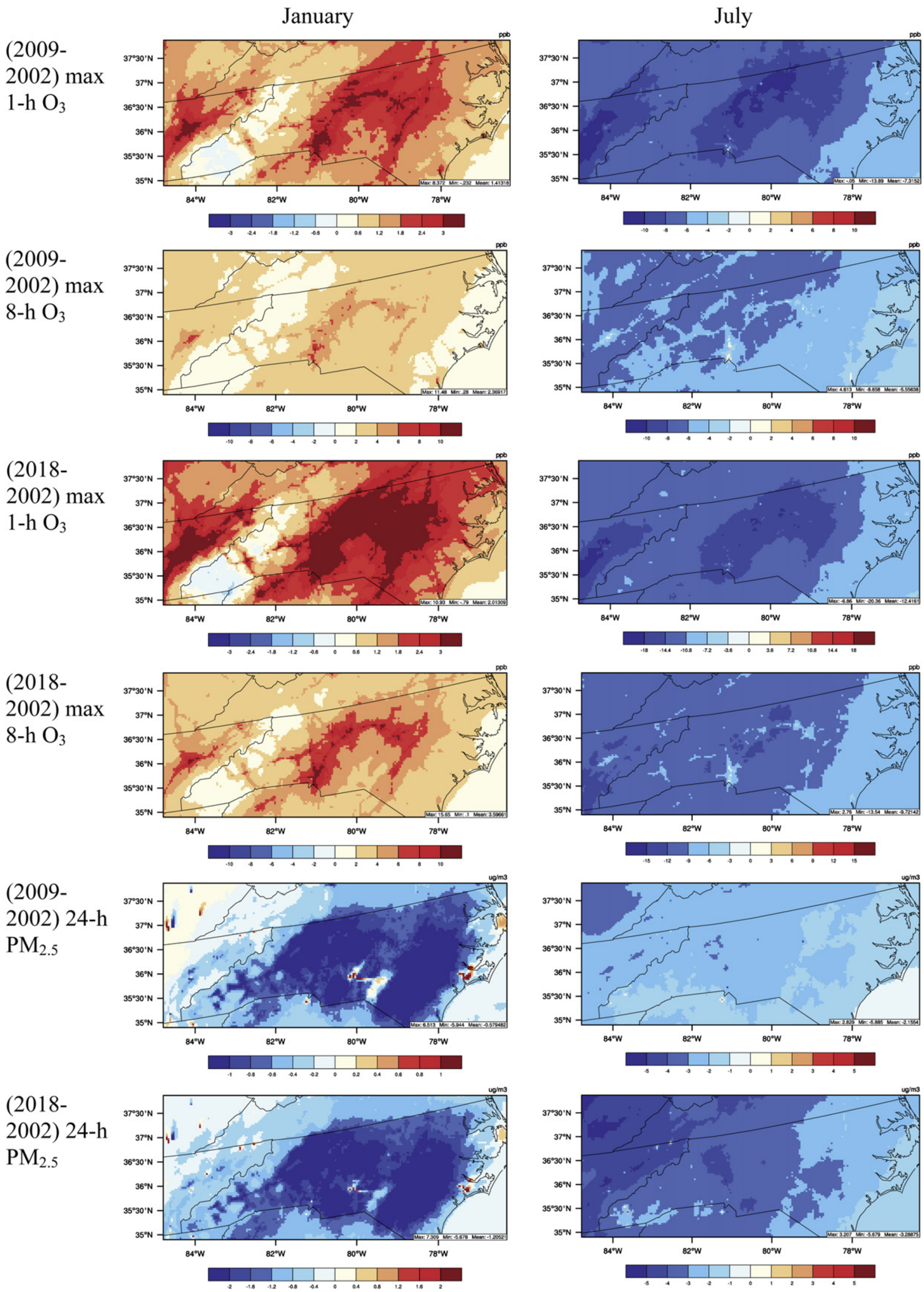

Fig. 2. Absolute differences in monthly-mean max 1-h and 8-h O_3 mixing ratios and 24-h average $PM_{2.5}$ concentrations simulated at the 4-km horizontal grid resolution in January and July 2002, 2009, and 2018.

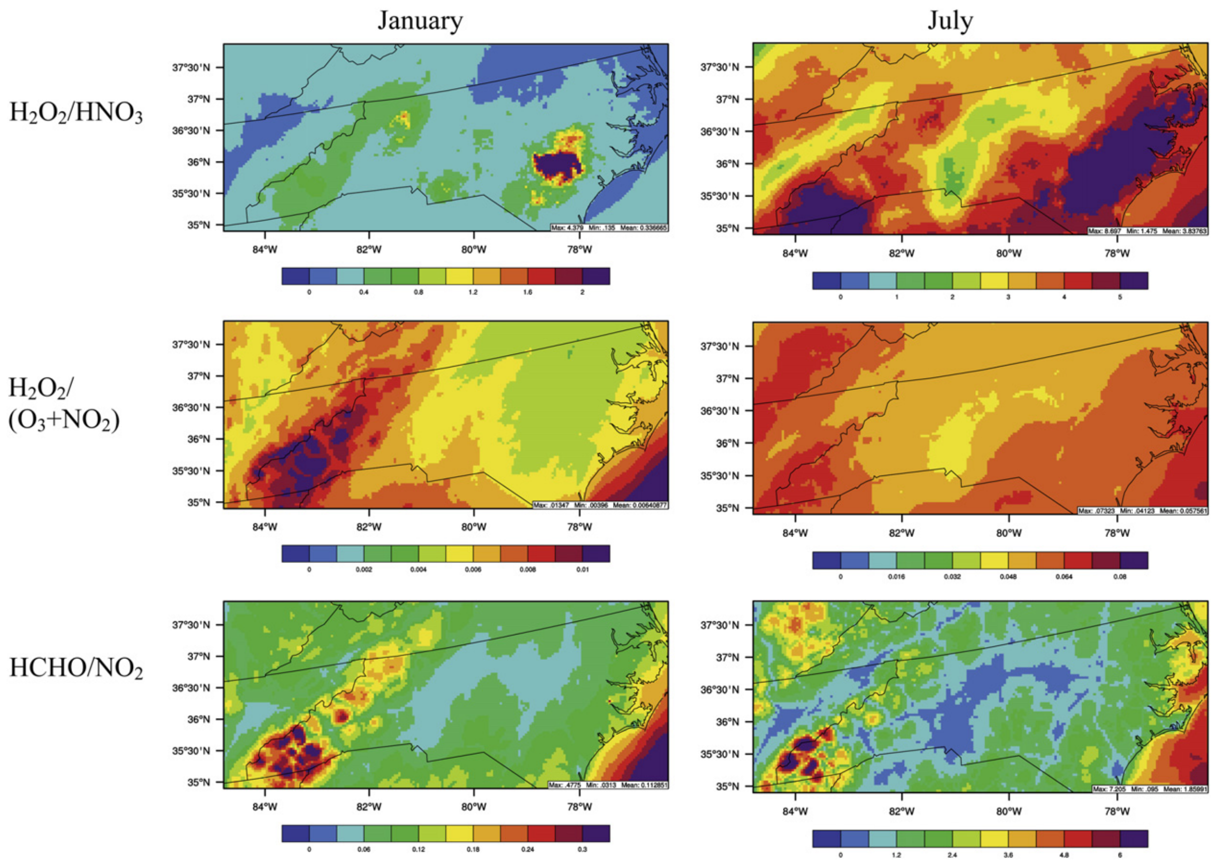

Fig. 3. Spatial distribution of Indicators in July and January, 2002, (a) H_2O_2/HNO_3, (b) $H_2O_2/(O_3 + NO_2)$, and (c) $HCHO/NO_2$.

the wet deposition amount of NH_4^+ increases by 2–10 mg ha^{-1} (2–10%) and 10–32 mg ha^{-1} (6–18%), respectively, over most of the domain, with the largest increases occurring in the mountain and Piedmont areas. By contrast, the wet deposition amount decreases by 200–600 mg ha^{-1} (16–32%) and 400–1000 mg ha^{-1} (28–50%), respectively, for SO_4^{2-} and 200–1000 mg ha^{-1} (10–40%) and 400–1500 mg ha^{-1} (28–56%), respectively, for NO_3^-. The variation trends in July 2009 and 2018 are somewhat different. The wet deposition amount of NH_4^+ increases by 2–50 mg ha^{-1} (2–10%) and 2–64 mg ha^{-1} (2–20%) in the central NC and some coastal areas but decreases by 2–50 mg ha^{-1} (2–10%) and 2–100 mg ha^{-1} (2–20%), respectively, in the remaining areas. The wet deposition amount decreases by 100–500 mg ha^{-1} (28–60%) and 100–1000 mg ha^{-1} (40–80%), respectively, for SO_4^{2-} and 400–2000 mg ha^{-1} (14–60%) and 600–5000 mg ha^{-1} (36–72%), respectively, for NO_3^-. While the reduction in the wet deposition amounts of SO_4^{2-} and NO_3^- is resulted from the reduction of their precursor emissions, the variation trend in the wet deposition amounts of NH_4^+ are dictated by the net effect of increased NH_3 emissions and either increased or decreased ambient concentrations of NH_4^+ as a result of thermodynamic equilibrium among inorganic salts in the atmosphere.

3. The sensitivity of model predictions to horizontal grid resolution

The sensitivity of model predictions to horizontal grid resolution in 2009/2018 simulations is overall similar. Fig. 7 shows absolute differences in the monthly-mean maximum 1-h and 8-h O_3 mixing ratios, 24-h average concentrations in $PM_{2.5}$, and EXT_Recon and DCV_Recon between the 4- and 12-km simulations in January and July 2009. Compared with the 12-km simulation, the 2009 4-km simulation gives higher O_3 (mostly 1–4 ppb, or < 10%, up to 6.6 ppb or 22.6%) in the mountain area but lower values (mostly 1–5 ppb, or < 20%, up to 17.6 ppb or 57.8%) in the central and coastal NC in January 2009. Similar trends are found for 2009 July simulations with less increase (mostly by 1–2 ppb, or < 4%) in a smaller area than January and also less decrease (mostly by 1–4 ppb, or 4–12%) in central and coastal areas. Compared with changes in the O_3 mixing ratios in 2009 relative to 2002, the increase is greater (mostly 1–5 ppb, or < 12%, up to 6.9 ppb or 26.3%) in January 2018 and the decrease is smaller in the central NC in July 2018 (Figure not shown). Contrary to trends in O_3, the 2009 January 4-km simulation generally gives higher $PM_{2.5}$ (mostly < 2 μg m^{-3}, or < 15%, up to 13.7 μg m^{-3} or 148.5%) in most Piedmont and coastal plain areas but lower values (mostly 0.5–2 μg m^{-3}, or < 20%, up to 4.13 μg m^{-3} or 49%) in the mountain areas than those at 12-km. Compared with 12-km results in July, the 4-km simulation gives higher values (mostly within 1 μg m^{-3} or 15%) in the mountain areas in KY, VA, and TN and the coastal plain area in NC but slightly lower values (mostly within 0.6 μg m^{-3} or 10%) in the Piedmont area. Larger cold bias in temperature predictions at 4-km than 12-km can help explain partially the higher values in January over most of the domain; higher precipitation and lower temperature may contribute in part to the lower values in July over most of the domain. The differences in $PM_{2.5}$ concentrations between the 2018 and 2002 January simulations are very similar to those between 2009 and 2002 in terms of spatial distribution and magnitude. For July simulation, less increase occurs in the mountain area and less decrease occurs in the Piedmont area, but larger increase occurs in the coastal plain area. For EXT_Recon and

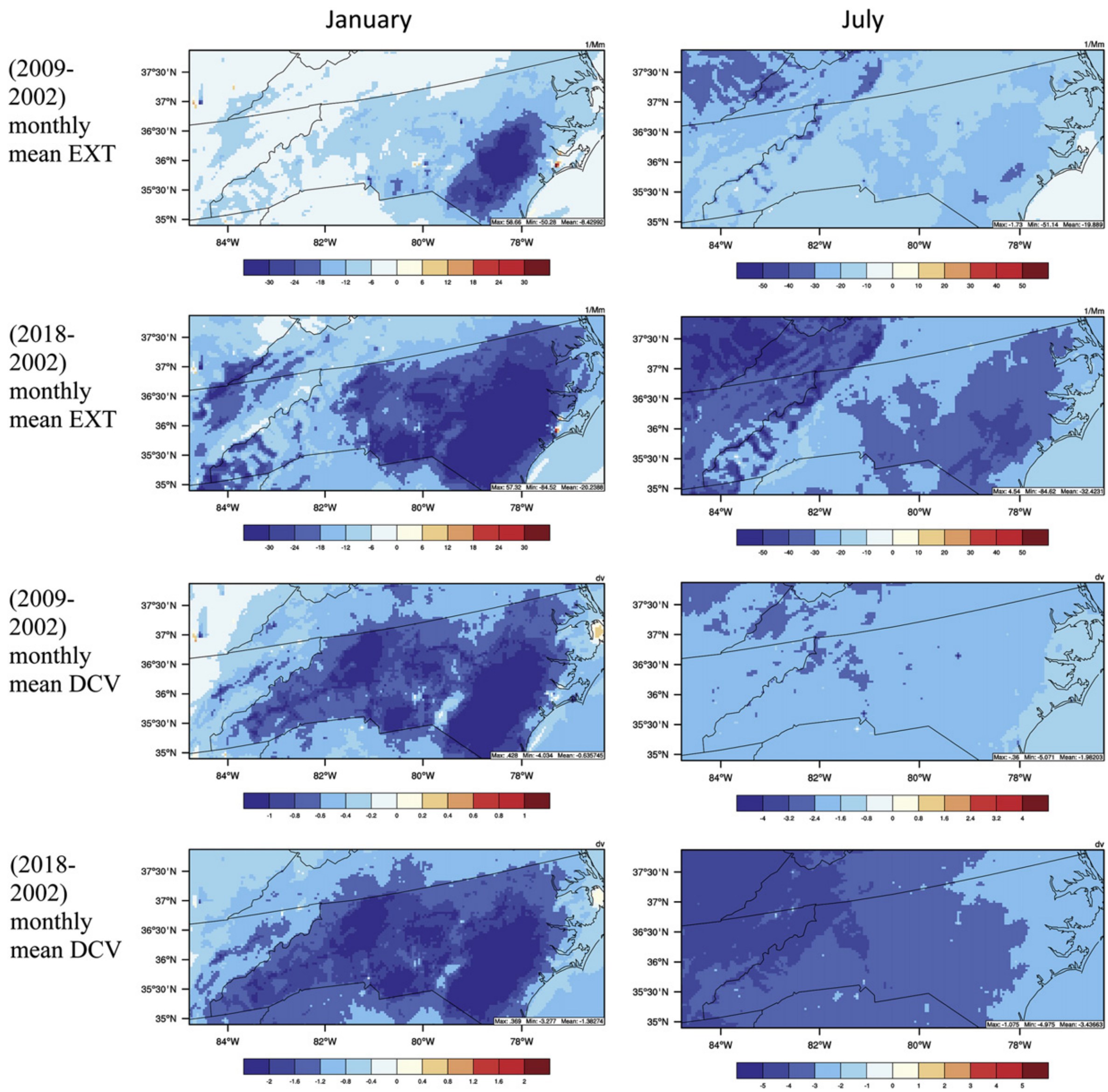

Fig. 4. Absolute differences in monthly-mean hourly EXT_Recon and DCV_Recon simulated at the 4-km horizontal grid resolution in January and July 2002, 2009, and 2018.

DCV_Recon in 2009 and 2018, the highest sensitivity is found in the mountain and the coastal plain areas with higher values at 4-km in January and slightly lower values at 4-km throughout the domain in July for the same reasons as differences in $PM_{2.5}$ predictions between 12- and 4-km simulation results. Fig. 8 shows absolute differences in the monthly-mean hourly total depositions of NH_4^+, SO_4^{2-}, and NO_3^- between the 4- and 12-km simulations in January and July 2009 (figure not shown for 2018 because of its similarity to that in 2009). Both dry and wet deposition amounts are highly sensitive to horizontal grid resolution, resulting in a high sensitivity in the total deposition amounts throughout the domain. While the dry deposition amounts exhibit high sensitivity in the mountain and coastal plain areas, the wet deposition amounts show high sensitivity throughout the domain. Such a high sensitivity is expected because of the strong dependence of dry and wet deposition on processes/parameters that are highly dependent on horizontal resolution such as land use, cloud/precipitation, and aqueous-phase chemistry. Compared with the 12-km results, the 4-km simulation gives 0.01–1000 mg ha^{-1} (up to 600%), 10–4000 mg ha^{-1} (up to 260%), and 10–2000 mg ha^{-1} (up to 400%) higher total deposition for NH_4^+, SO_4^{2-}, and NO_3^-, respectively, in January 2009. It gives 0.1–1000 mg ha^{-1} (up to 490%), 10–5000 mg ha^{-1} (up to 300%), and 10–1000 mg ha^{-1} (up to 470%) higher values in the mountain and coastal plain areas but 0.01–1000 mg ha^{-1} (up to 95%), 10–6000 mg ha^{-1} (up to 94%), and 10–800 mg ha^{-1} (up to 96%) lower values in many regions for NH_4^+, SO_4^{2-}, and NO_3^-, respectively, in July 2009.

While the impacts of grid resolution on model predictions in 2009 and 2018 are similar to those in 2002, the discrepancies in simulated maximum 1-h and 8-h O_3 mixing ratios, 24-h average concentrations of $PM_{2.5}$ and its components, and dry and wet deposition amounts between the two grid resolutions for January 2002 are overall larger than those in 2009 and 2018, indicating the current-year simulation is slightly more sensitive to grid resolution in winter.

4. Modeled attainment test

The U.S. EPA's modeled attainment test is performed to estimate the impact of emission controls in 2009/2018 on the attainment of 8-h average max O_3 and 24-h average $PM_{2.5}$ at a given monitor over NC.

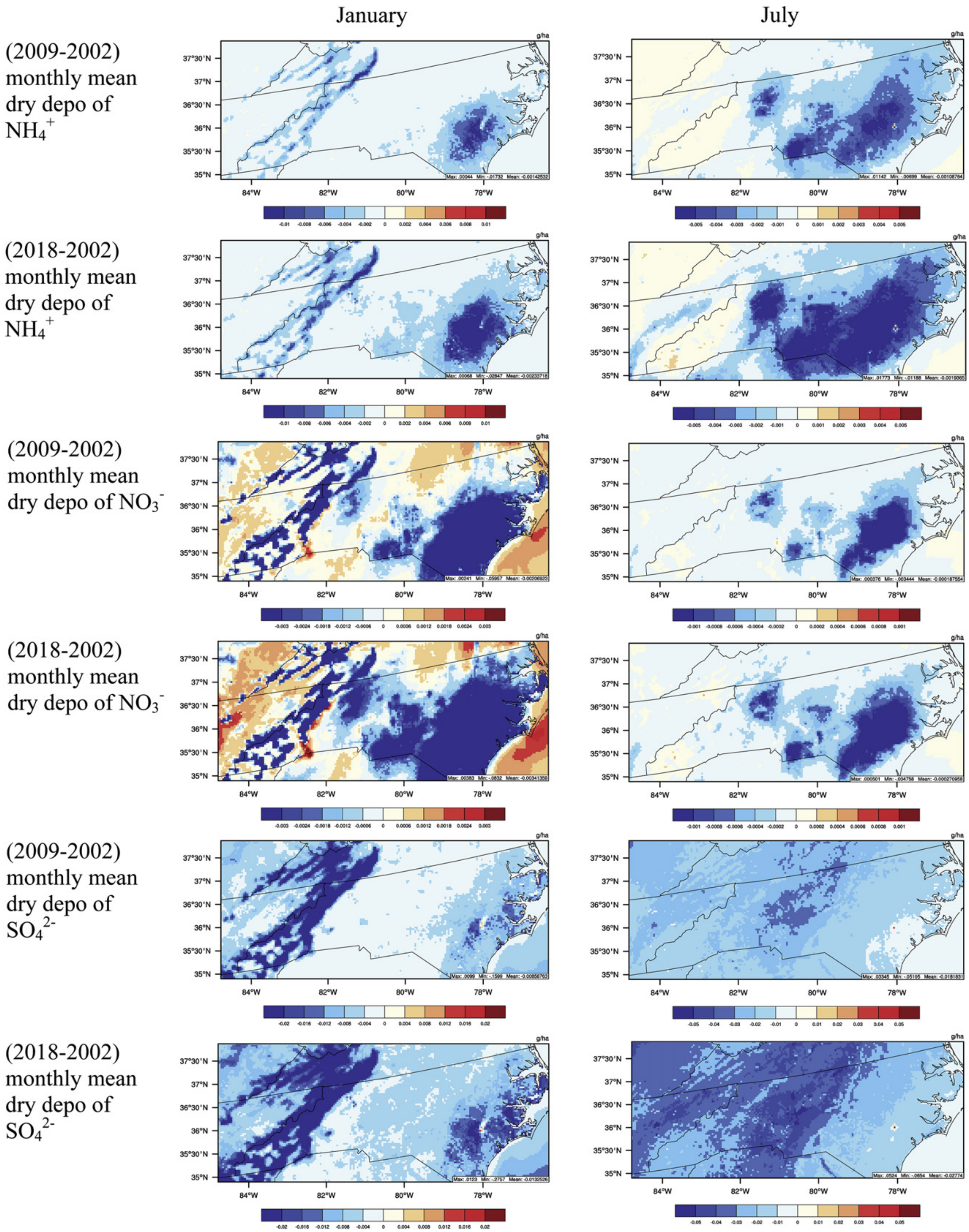

Fig. 5. Absolute differences in monthly-mean hourly dry deposition amounts of $PM_{2.5}$ NH_4^+, SO_4^{2}, and NO_3^- simulated at the 4-km horizontal grid resolution in January and July 2002, 2009, and 2018.

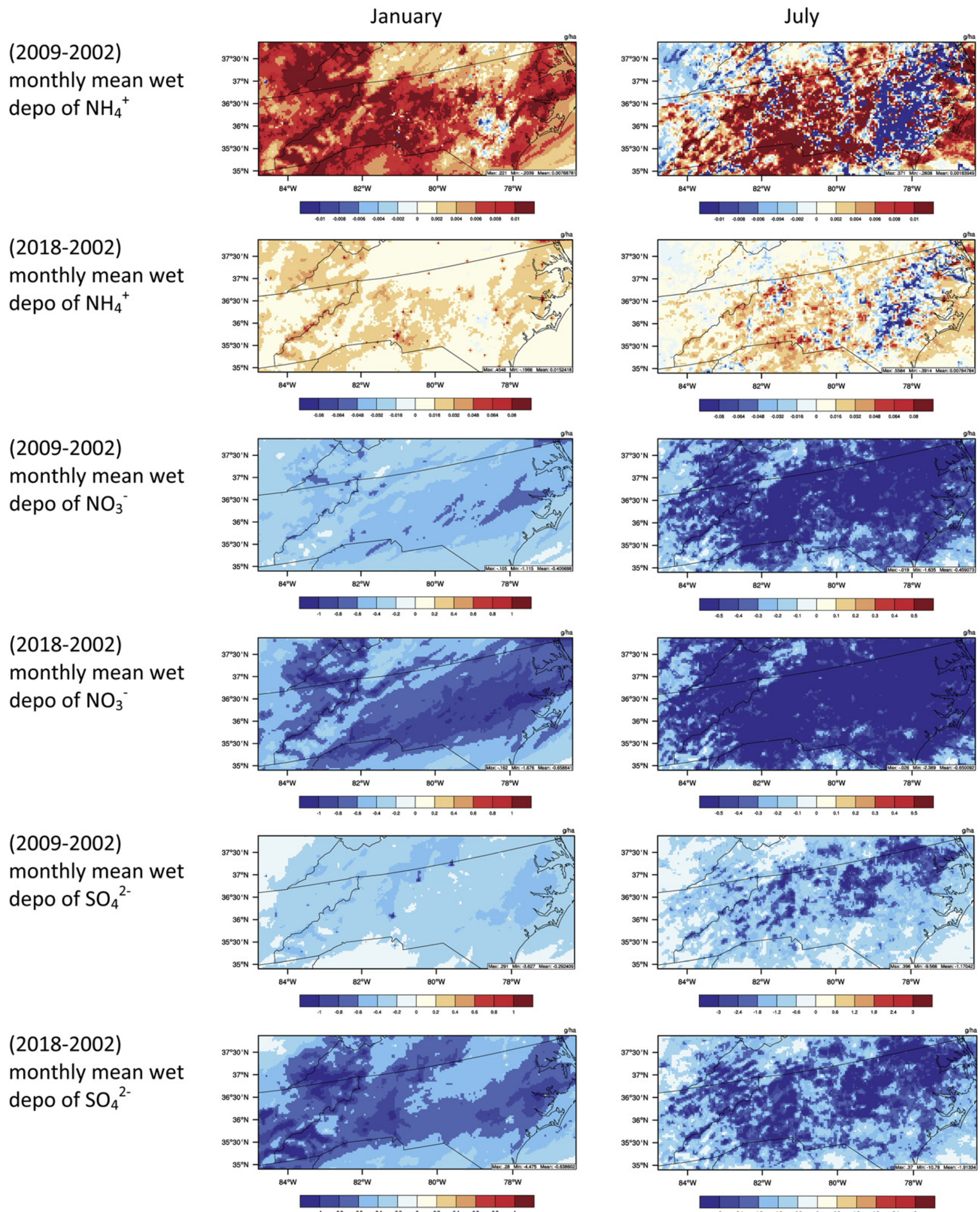

Fig. 6. Absolute differences in monthly-mean hourly wet deposition amounts of $PM_{2.5}$ NH_4^+, SO_4^{2-}, and NO_3^- simulated at the 4-km horizontal grid resolution in January and July 2002, 2009, and 2018.

The results are summarized in Tables 1–3. The site-specific current design values (DVCs) for 8-h max O_3 are obtained from NCDENR, except for four CASTNET sites where those values are obtained from Arunachalam et al. (2006). The DVCs were calculated as 5-year weighted design values at each site based on the 4th-highest daily maximum 8-h O_3 concentrations during 2000–2004. Those for 24-h average $PM_{2.5}$ are also obtained from NCDENR; they are calculated based on the average of quarterly design values of 24-h average $PM_{2.5}$ concentrations at each site during 2000–2004. The results from the 4-km and 12-km 2002 June, July, and August simulations

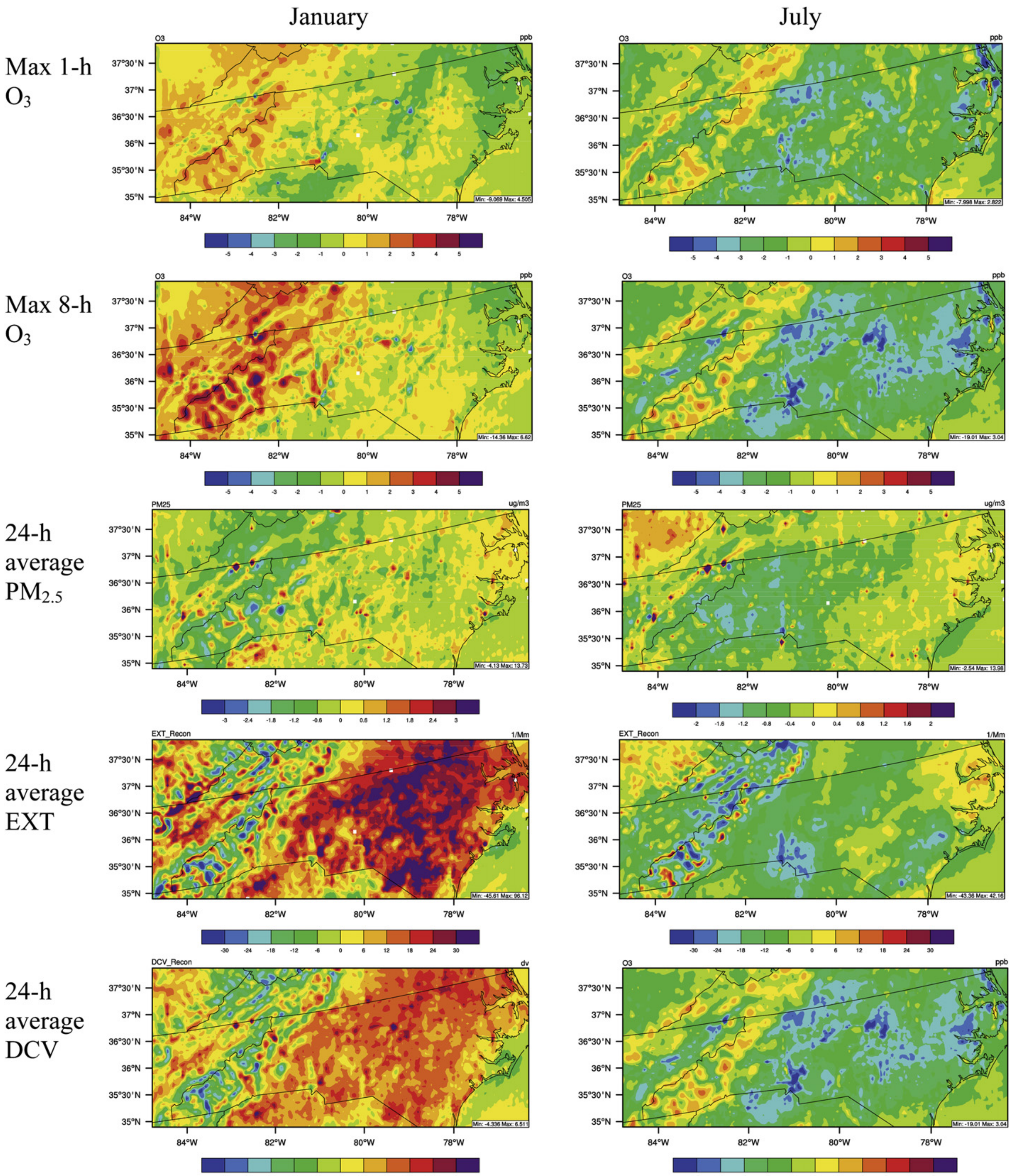

Fig. 7. Absolute differences in max 1-h and 8-h O_3 mixing ratios, 24-h average $PM_{2.5}$, 24-h average EXT_Recon, and 24-h average DCV_Recon simulated at the 4- and 12-km horizontal grid resolutions in January and July, 2009.

with "typical" emissions are used to estimate the site-specific relative reduction factor (RRF), which equals to the ratio of the mean base-year value (Mean_BY) to the mean future-year value (Mean_FY), as well as the site-specific future-year design value (DVF). The U.S. EPA's recommended O_3 modeled attainment test methodology (U.S. EPA, 2007) is used but only applied to the summer months (i.e., June, July, and August) and not an entire O_3 monitoring season (April through October for NC). For the $PM_{2.5}$ modeled

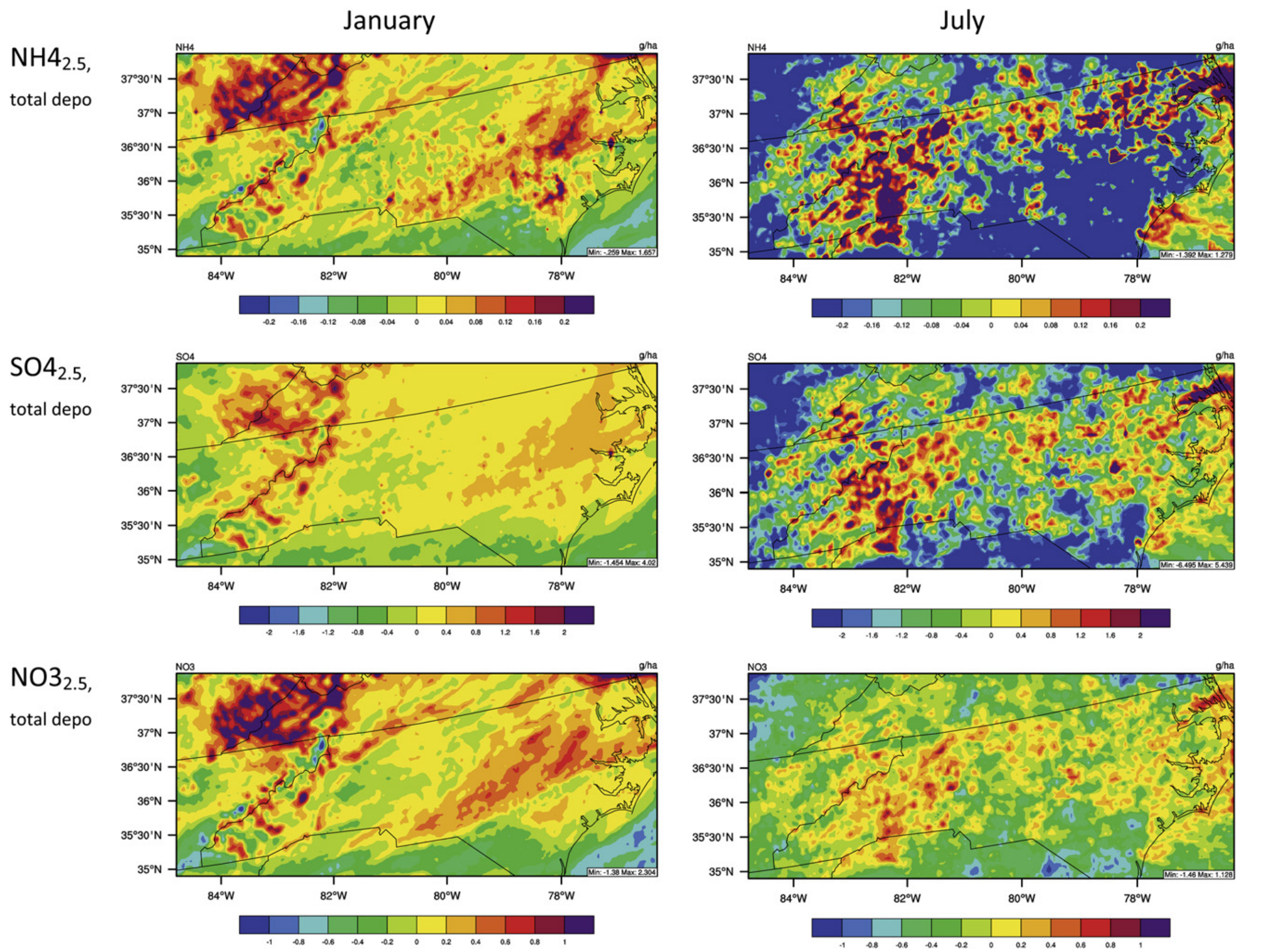

Fig. 8. Absolute differences in monthly-mean hourly total deposition amounts (in kg ha^{-1}) of ammonium, sulfate, and nitrate in $PM_{2.5}$ simulated at the 4- and 12-km horizontal grid resolutions in January and July, 2009.

attainment test, the $PM_{2.5}$ RRFs are calculated by taking the ratio of future year and base-year total $PM_{2.5}$ mass concentrations. The Speciated Model Attainment Test (SMAT) methodology recommended by the U.S. EPA is not used here because the observed mass concentrations during 2000–2004 at the Federal Reference Method (FRM) monitors are not available for all seven $PM_{2.5}$ species required by SMAT and the interpolation method to obtain the speciation data contains some uncertainties. SMAT is recommended for the $PM_{2.5}$ modeled attainment test when such speciation data are available in the future. To increase the representativeness of the model results for urban-scale O_3 and $PM_{2.5}$ monitors, a block of grid cells that are within 15-km radius of the monitor, rather than a single cell in which the monitor is located, are considered in calculating the RRFs and DVFs based on the method of Arunachalam et al. (2006). Each block consists of 7×7 and 3×3 grid cells (with the monitor in the center cell) for the 4-km and 12-km simulations, respectively. Following Arunachalam et al. (2006), only the days when the highest 8-h max O_3 value was ≥ 0.070 ppm are considered.

For 8-h max O_3 DVCs, 49 out of 50 sites (except at Bryson City) are in non-attainment, having a concentration >0.075 ppm. For 2009 8-h max O_3 DVFs, all sites in Charlotte, several sites in Triangle, Triad, and Asheville areas, and one site in the Greenville, Rocky Mount and Wilson area and in the NW Piedmont will be in the non-attainment (23 and 16 out of a total of 50 sites in NC based on both 4- and 12-km simulations, respectively). For 2018 8-h max O_3 DVFs, only 1 site in Charlotte (i.e., Garinger) is in non-attainment at 4-km and all sites are in attainment at 12-km. Comparing the 4-km RRFs with the 12-km RRFs, 7 and 23 sites of the 50 sites have $>3\%$ differences in 2009 and 2018, respectively. The differences between the 4-km RRFs with the 12-km RRFs correspond to 1–3.8 ppb at 23 sites in 2009 and 1.1–6.0 ppb at 31 sites in 2018. The Student's *t*-test is performed to determine whether the daily RRFs for the 12- and 4-km simulations are equal, which further helps isolate areas that may benefit from fine grid resolution (Arunachalam et al., 2006). A p-value < 0.05 indicates a significant difference between RRFs for the 12- and 4-km simulations. The detailed statistical theory for Student's *t*-test was described in Arunachalam et al. (2006). None of the 50 sites in 2009/2018 have significantly different RRFs for 8-h max O_3 simulated at 12- and 4-km, indicating that the simulated 8-h max O_3 is relatively insensitive to horizontal grid resolution and a 12-km grid resolution may be sufficient for O_3 modeling in support of SIPs in NC.

For 24-h $PM_{2.5}$ DVCs, only 1 out of a total of 37 sites (i.e., the 1st Street in NW Piedmont) is in non-attainment, having a concentration >35 μg m^{-3}. For 2009 24-h $PM_{2.5}$ DVFs, all sites are in the attainment based on both 4- and 12-km simulations. For 2018 24-h $PM_{2.5}$ DVFs, all sites are in attainment based on the 4-km simulation. Comparing the 4-km RRFs with the 12-km RRFs, 12 and 5 sites have 3–5% and $>5\%$ differences, respectively, in 2009 and 3 and 33 sites have 3–5% and $>5\%$ differences in 2018. These differences correspond to 1.1–4.5 μg m^{-3} at 6 sites in 2009 and 1.1–7.9 μg m^{-3} at 32 sites in 2018. 11 sites in 2009 and 31 sites in 2018 have p-values < 0.05, indicating significantly

Table 1
O_3 design values and p-values from student's t-test.

AIRS ID	Site ID	Site name	DVC[a]	2009DVF		2018DVF		p-values(12 km vs. 4 km)	
				4 km	12 km	4 km	12 km	2009	2018
Charlotte									
37-119-1009	CTYL	CountyLine	0.0973	0.0847	0.0842	0.0737	0.0716	0.974	0.977
37-159-0021	ROCK	Rockwell	0.0973	0.0841	0.0831	0.0739	0.0714	0.942	0.957
37-159-0022	ENVL	Enochville	0.0970	0.0839	0.0839	0.0739	0.0715	0.995	0.997
37-119-0041	PLZA	Garinger (Plaza)	0.0953	0.0853	0.0840	0.0766	0.0728	0.915	0.938
37-109-0004	CRSE	Crouse	0.0907	0.0788	0.0779	0.0694	0.0683	0.943	0.955
37-119-1005	ARWD	Arrowood	0.0847	0.0757	0.0742	0.0678	0.0642	0.917	0.939
37-179-0003	MONR	Monroe	0.0870	0.0752	0.0761	0.0651	0.0652	0.955	0.947
Triangle (Raleigh-Durham-Chapel Hill)									
37-183-0014	MLBK	Millbrook	0.0907	0.0794	0.0790	0.0681	0.0675	0.978	0.984
37-077-0001	BTNR	Butner	0.0923	0.0780	0.0790	0.0672	0.0683	0.954	0.947
37-183-0015	STAG	St. Augustine	0.0927	0.0809	0.0808	0.0688	0.0690	0.992	0.995
37-145-0003	BSHF	Bushy Fork	0.0893	0.0747	0.0731	0.0665	0.0632	0.945	0.930
37-069-0001	FRKL	Franklinton	0.0897	0.0771	0.0776	0.0664	0.0665	0.974	0.979
37-063-0013	DUKE	DUKE Duke St.	0.0887	0.0764	0.0766	0.0658	0.0654	0.990	0.992
37-183-0017	WRAL	Tower	0.0853	0.0743	0.0741	0.0638	0.0633	0.987	0.992
37-183-0016	FUQV	Fuquay-Varina	0.0873	0.0759	0.0741	0.0638	0.0633	0.987	0.992
37-101-0002	WJOH	W. Johnston	0.0843	0.0715	0.0726	0.0601	0.0611	0.933	0.964
37-037-0004	PITT	Pittsboro	0.0813	0.0695	0.0705	0.0605	0.0609	0.945	0.964
Triad (Greensboro-Winston-Salem-High Point)									
37-059-0002	DAVI	Cooleemee	0.0913	0.0787	0.0773	0.0700	0.0664	0.917	0.935
37-067-0022	HTAV	Hattie Ave.	0.0913	0.0766	0.0754	0.0678	0.0649	0.952	0.951
37-067-1008	UCRS	Union Cross	0.0883	0.0758	0.0745	0.0658	0.0641	0.936	0.950
37-157-0099	BETH	Bethany	0.0883	0.0752	0.0713	0.0671	0.0611	0.854	0.811
37-033-0001	CHGR	Cherry Grove	0.0877	0.0741	0.0731	0.0643	0.0626	0.954	0.944
37-081-0011	MLVL	McLeansville	0.0887	0.0778	0.0756	0.0675	0.0641	0.885	0.905
37-067-0028	SHIL	ShilohChurch	0.0863	0.0719	0.0712	0.0639	0.0618	0.976	0.973
37-151-0004	SOPH	Sophia	0.0850	0.0729	0.0727	0.0633	0.0624	0.988	0.991
37-067-0027	POLL	Pollirosa	0.0817	0.0675	0.0681	0.0605	0.0596	0.978	0.977
Asheville									
37-199-0003	MTMI	Mt.Mitchell	0.0827	0.0733	0.0727	0.0660	0.0648	0.962	0.981
37-087-0035	FRYP	Fry Pan	0.0823	0.0752	0.0734	0.0699	0.0671	0.929	0.954
37-087-0036	PKNO	Purchase Knob	0.0847	0.0761	0.0738	0.0696	0.0663	0.875	0.927
37-099-0005	BKNO	Barnet Knob	0.0833	0.0753	0.0737	0.0688	0.0666	0.917	0.956
37-021-0030	BENT	Bent Creek	0.0800	0.0712	0.0690	0.0645	0.0607	0.856	0.913
37-087-0004	WAYN	Waynesville	0.0783	0.0707	0.0693	0.0655	0.0632	0.908	0.947
37-173-0002	BRYS	Bryson City	0.0730	0.0657	0.0634	0.0599	0.0556	0.923	0.948
Greenville, Rocky Mount and Wilson (Down East)									
37-065-0099	LEGT	Leggett	0.0873	0.0755	0.0757	0.0686	0.0652	0.987	0.994
37-147-0099	FARM	Farmville	0.0820	0.0698	0.0708	0.0604	0.0606	0.949	0.979
37-107-0004	KINS	L. College	0.0800	0.0668	0.0699	0.0575	0.0607	0.855	0.931
37-061-0002	KVIL	Kenansville	0.0800	0.0677	0.0708	0.0683	0.0626	0.862	0.953
37-117-0001	JVIL	Jamesville	0.0810	0.0733	0.0718	0.0689	0.0632	0.921	0.959
Fayetteville									
37-051-0008	WADE	Wade	0.0853	0.0725	0.0731	0.0608	0.0619	0.967	0.982
37-051-1003	HOPE	Golfview	0.0860	0.0739	0.0741	0.0625	0.0628	0.986	0.992
NW Piedmont(Hickory)									
37-003-0003	ALEX	Taylorsville	0.0870	0.0767	0.0755	0.0681	0.0661	0.899	0.939
37-027-0003	LENR	Lenoir	0.0833	0.0739	0.0734	0.0663	0.0647	0.955	0.979
Various areas									
37-131-0002	GAST	Gaston	0.0853	0.0742	0.0740	0.0713	0.0664	0.993	0.996
37-029-0099	CAMD	Camden	0.0777	0.0698	0.0696	0.0640	0.0632	0.978	0.989
37-011-0002	LINV	Linville	0.0777	0.0692	0.0690	0.0635	0.0628	0.983	0.991
37-129-0002	WILM	Castle Hayne	0.0773	0.0693	0.0695	0.0622	0.0613	0.992	0.994
CASTNET Sites									
37-123-8001	CAND	Candor	0.086	0.0741	0.0750	0.0644	0.0647	0.936	0.940
37-011-8001	CRAN	Cranberry	0.083	0.0745	0.0741	0.0688	0.0672	0.978	0.988
37-113-8001	COWE	Coweeta	0.077	0.0700	0.0677	0.0625	0.0597	0.924	0.956
37-031-8001	BEAU	Beaufort	0.076	0.0675	0.0680	0.0617	0.0610	0.963	0.981

[a] The DVC values for the CASTNET sites are taken from Arunachalam et al. (2006), and for other sites are provided by NCDENR.

different RRFs for 24-h average $PM_{2.5}$ simulated at the 12- and 4-km. This indicates that the simulated 24-h average $PM_{2.5}$ for future years is sensitive to horizontal grid resolution and a 12-km grid resolution may not be sufficient for daily $PM_{2.5}$ modeling in support of SIPs in NC.

5. Summary

MM5/CMAQ simulations are conducted to simulate air quality of January and July 2002, 2009, and 2018. The impact of planned emission control strategies are examined to evaluate their

Table 2
$PM_{2.5}$ design values and *p*-values from student's *t*-test.

AIRS ID	Site name	DVC[a]	2009DVF		2018DVF		*p*-values(12 km vs. 4 km)	
			4 km	12 km	4 km	12 km	2009	2018
Charlotte								
37-025-0004	Floyd	32	25.396	25.000	21.817	20.718	0.332	0.020
37-119-0010	Remount	32	23.947	26.983	27.982	22.658	0.000	0.000
37-119-0041	Eastway	30	22.418	25.325	26.229	21.274	0.000	0.000
37-119-0042	Emerywood	30	22.463	25.325	26.273	21.274	0.000	0.000
Triangle (Raleigh-Durham-Chapel Hill)								
37-037-0004	Russett Run	27	21.290	20.546	18.746	17.316	0.022	0.002
37-063-0001	Main St.	33	23.468	26.725	27.874	23.813	0.000	0.000
37-135-0007	Mason Farm	29	23.380	22.798	21.100	19.701	0.066	0.004
37-183-0014	Spring Forest	32	26.787	26.520	24.406	23.775	0.452	0.224
37-183-0015	North Street	33	27.528	27.349	25.358	24.518	0.628	0.115
Triad (Greensboro-Winston-Salem-High Point)								
37-001-0002	S. Graham & Hopedale	32	24.538	24.017	21.524	20.383	0.181	0.020
37-033-0001	Cherry Grove	33	24.906	24.587	21.688	20.820	0.452	0.087
37-057-0002	S.SALISBURY	35	27.511	26.826	23.990	22.676	0.080	0.007
37-067-0022	Hattie	34	26.382	25.491	23.308	21.674	0.030	0.001
37-067-0024	NORTH FORSYTH	35	26.543	25.821	23.317	21.524	0.119	0.001
37-081-0009	Edgeworth&Bellemeade	26	20.108	19.977	18.242	16.983	0.656	0.001
37-081-0013	Wiloughby	28	21.597	21.254	19.574	18.050	0.307	0.000
Asheville								
37-087-0010	9 Main St.	28	22.151	21.252	18.603	16.761	0.006	0.000
37-099-0006	US Route 19	29	21.891	23.040	17.172	19.974	0.339	0.167
37-121-0001	City Hall Summit	30	22.692	22.372	18.275	17.334	0.442	0.016
37-173-0002	Center St.	28	27.280	22.771	27.761	19.899	0.391	0.354
37-021-0034	Bingham	30	24.422	23.485	21.557	19.185	0.021	0.000
Greenville, Rocky Mount and Wilson (Down East)								
37-061-0002	Kenansville	27	22.114	21.343	22.850	18.366	0.178	0.000
37-065-0003	Talbert Park	30	24.325	23.610	24.302	20.746	0.106	0.000
37-107-0004	Highway east	26	20.942	20.471	19.742	17.497	0.231	0.001
37-147-0005	Howell	28	22.297	21.984	20.481	19.033	0.429	0.026
37-191-0005	Devereau St.	29	23.664	22.764	21.878	19.425	0.000	0.001
Fayetteville								
37-051-0009	Raeford	31	25.026	24.289	22.440	20.527	0.057	0.001
37-155-0005	Linkhaw	27	22.535	21.616	20.275	18.378	0.019	0.002
NW Piedmont(Hickory)								
37-035-0004	1st St.	38	29.556	28.883	24.911	23.269	0.238	0.005
Various areas								
37-071-0016	East Garrison	29	23.745	23.720	20.676	19.421	0.943	0.003
37-111-0004	Balwin	30	23.306	22.553	19.213	17.694	0.065	0.000
37-129-0002	Holly Shelter	23	19.719	19.830	18.138	17.020	0.655	0.005
37-129-0009	Market	24	20.655	20.868	19.168	18.094	0.372	0.007
37-133-0005	Henderson	25	20.598	20.342	18.444	17.160	0.453	0.017
37-139-0002	Westover St.	29	23.910	23.098	22.380	20.680	0.049	0.004
37-123-0001	Perry	26	20.090	19.777	17.503	16.396	0.308	0.007
37-189-0003	Jefferson	30	22.624	22.344	17.907	17.205	0.514	0.076

[a] The DVC values are based on the max of the observed 24-average $PM_{2.5}$ concentrations at each site during 2000–2004.

Table 3
Number of sites that have differences in 12-km RRFs compared to 4-km.

Magnitude of RRF difference (%)	2009	2018
(a) Max 8 h O_3		
0	0	0
<1	21	11
1–2	15	11
2–3	7	5
>3	7	23
(b) 24 h average $PM_{2.5}$		
0	0	0
<1	4	0
1–3	15	1
3–5	12	3
>5	5	33

effectiveness in controlling $PM_{2.5}$ and O_3 levels in NC in 2009 and 2018. The impact of horizontal grid resolution on simulated O_3 and $PM_{2.5}$ and their policy implications are assessed. The planned emission control strategy will reduce O_3 levels by up to 22.5% in July 2009/2018 from its level in 2002. It will, however, cause 3.7% and 5.3% increase in the max 1-h O_3 and 7.3% and 11.2% increase in the max 8-h O_3 in 2009 and 2018, respectively, due to the VOC-limited O_3 chemistry in winter in the southeastern U.S. While the simulated max 1-h and 8-h O_3 mixing ratios in 2009 and 2018 are relatively insensitive to horizontal grid resolution, the simulated concentrations of $PM_{2.5}$ and its components, visibility indices, and dry and wet deposition amounts in 2009/2018 are highly sensitive to horizontal grid resolution. Such sensitivity or insensitivity is expected due to different levels of dependence on parameters/processes that are affected by horizontal grid resolution.

The U.S. EPA's modeled attainment test shows that the projected emission control for simulations at 4-km will reduce the number of sites in non-attainment for max 8-h O_3 from 49 to 23 in 2009 and to 1 in 2018 and for 24-h average $PM_{2.5}$ from 1 to 0 in 2009 and 2018 based on the latest 2008 $O_3$and 2006 $PM_{2.5}$ NAAQSs. 23 sites out of 50 sites have >3% differences in RRFs for max 8-h O_3 in 2018. The differences in max 8-h O_3 RRFs translate to an average difference of 1–3.8 ppb at 23 sites in 2009 and 1.1–6.0 ppb at 31 sites in 2018, generally consistent with results from Arunachalam et al. (2006). 12 and 5 sites have 3–5% and >5% differences, respectively, in 24-h average $PM_{2.5}$ RRFs in 2009 and 3 and 33 sites have 3–5% and >5% differences in 2018. The differences in 24-h average $PM_{2.5}$ RRFs translate to an average difference of 1.1–4.5 $\mu g\ m^{-3}$ at 6 sites in 2009 and 1.1–7.9 $\mu g\ m^{-3}$ at 32 sites in 2018. The Student's *t*-test shows that simulated 8-h max O_3 is insensitive but simulated 24-h average $PM_{2.5}$ is quite sensitive to horizontal grid resolution, indicating potential differences in daily $PM_{2.5}$ SIPs developed based on results at 4- and 12-km. Note that the sensitivity to grid resolution may vary from one region to another. Whether to use 4-km or 12-km for SIP modeling depends on such sensitivity studies and the availability of computational resources for simulations at a finer scale.

In addition to emission controls, meteorological variables and their changes will affect future air quality predictions. For example, meteorological dispersion rates will affect the sensitivity of O_3 to its precursors, NO_x, and VOCs (Sillman et al., 1990). Temperature, humidity, and clouds have impacts on PM formation (Zhang et al., 2008; Leung and Gustafson, 2005; Hogrefe et al., 2004; Tagaris et al., 2007). The impact of climate change is not included in the future-year simulations conducted in this work. The differences in climate between 2009/2018 and 2002 may not be sufficiently robust to demonstrate the changes in climate and their impact on simulated air quality that would typically require a longer time frame (e.g., 30–50 years between 2030 and 2050 and 2000). Such an impact along with the impact of emission changes should be evaluated in future study.

Acknowledgements

This work was supported by North Carolina Department of Environment and Natural Resources Division of Air Quality, the USDA Air Quality Program/National Research Initiative Competitive Grant no. 2008-35112-18758, and the National Science Foundation Career Award Atm-0348819. Thanks are due to Mike Abraczinskas, Chris Misenis, Wayne Cornelius, Karen Harris, and Hoke Kimball of NCDENR for providing VISTAS's 12-km CMAQ inputs and results and observational data; Don Olerud, BAMS, for providing VISTAS's 12-km MM5 results.

References

Arunachalam, S., Holland, A., Do, B., Abraczinskas, M., 2006. A quantitative assessment of the influence of grid resolution on predictions of future-year air quality in North Carolina, USA. Atmospheric Environment 40, 5010–5026.

Hogrefe, C., Lynn, B., Civerolo, K., Ku, J.-Y., Rosenthal, J., Rosenzweig, C., Goldberg, R., Gaffin, S., Knowlton, K., Kinney, P.L., 2004. Simulating changes in regional air quality over the eastern United States due to changes in global and regional climate and emissions. Journal of Geophysical Research 109, D22301. doi:10.1029/2004JD004690.

Jacob, D.J., Horowitz, L.W., Munger, J.W., Heikes, B.G., Dicherson, R.R., Artz, R.S., Keene, W.C., 1995. Seasonal transition from NO_x^- to hydrocarbon-limited conditions for ozone production over the eastern United States in September. Journal of Geophysical Research 100, 9315–9324.

Leung, L.R., Gustafson, W.I., 2005. Potential regional climate change and implications to US air quality. Geophysical Research Letters 32, L16711. doi:10.1029/2005GL022911.

Liao, H., Chen, W.-T., Seinfeld, J.H., 2006. Role of climate change in global predictions of future tropospheric ozone and aerosols. Journal of Geophysical Research 111, D12304. doi:10.1029/2005JD006852.

Liu, X.-H., Y. Zhang, J. Xing, Q. Zhang, D.G. Streets, C.J. Jang, W.-X. Wang, and J.-M. Hao. Understanding of regional air pollution over China using CMAQ: – Part II. Process analysis and ozone sensitivity to precursor emissions, Atmospheric Environment, in press a, doi:10.1016/j.atmosenv.2010.03.035.

Liu, X.-H., Zhang, Y., Olsen, K., Wang, W.-X., Do, B., Bridgers, G. Responses of future air quality to emission controls over North Carolina, Part I: Model evaluation for current-year simulations, Atmospheric Environment, in press b, doi:10.1016/j.atmosenv.2010.04.002.

Meng, Z., Dabdub, D., Seinfeld, J.H., 1997. Chemical coupling between atmospheric ozone and particulate matter. Science 277, 116–119.

Pinder, R.W., Gilliland, A.B., Dennis, R.L., 2008. Environmental impact of atmospheric NH_3 emissions under present and future conditions in the eastern United States. Geophysical Research Letters 35, L12808. doi:10.1029/2008GL033732.

Queen, A., Zhang, Y., 2008. Examining the sensitivity of MM5-CMAQ predictions to explicit microphysics schemes and horizontal grid resolutions, Part III-The impact of horizontal grid resolution. Atmospheric Environment 42, 3869–3881.

Sillman, S., 1995. The use of NO_y, H_2O_2, and HNO_3 as indicators for ozone-NO_x-hydrocarbon sensitivity in urban locations. Journal of Geophysical Research 100, 14175–14188.

Sillman, S., Logan, J.A., Wofsy, S.C., 1990. The sensitivity of ozone to nitrogen-oxides and hydrocarbons in regional ozone episodes. Journal of Geophysical Research 95, 1837–1851.

Tagaris, E.K., Manomaiphiboon, K., Liao, K.J., Leung, L.R., Woo, J.-H., He, S., Amar, P., Russell, G., 2007. Impacts of global climate change and emissions on regional ozone and fine particulate matter concentrations over the United States. Journal of Geophysical Research 112, D14312. doi:10.1029/2006JD008262.

Tonnesen, G.S., Dennis, R.L., 2000. Analysis of radical propagation efficiency to assess ozone sensitivity to hydrocarbons and NO_x 2. Long-lived species as indicators of ozone concentration sensitivity. Journal of Geophysical Research 105, 9227–9241.

Tsimpidi, A.P., Karydis, V.A., Pandis, S.N., 2007. Response of inorganic fine particulate matter to emission changes of sulfur dioxide and ammonia: the eastern United States as a case study. Journal of the Air & Waste Management Association 57, 1489–1498.

U.S. EPA, April, 2007. Guidance on the Use of models and Other Analyses for Demonstrating Attainment of Air Quality Goals for Ozone, PM2.5 and Regional Haze. U.S. Environmental Protection Agency, Research Triangle Park, NC. EPA-454/B-07–002.

Wu, S., Mickley, L.J., Leibensperger, E.M., Jacob, D.J., Rind, D., Streets, D.G., 2008a. Effects of 2000–2050 global change on ozone air quality in the United States. Journal of Geophysical Research 113, D06302. doi:10.1029/2007JD008917.

Wu, S.-Y., Krishnan, S., Zhang, Y., Aneja, V.P., 2008b. Modeling atmospheric transport and fate of ammonia in North Carolina-Part I: evaluation of meteorological and chemical predictions. Atmospheric Environment 42, 3419–3436.

Zhang, Y., Vijayaraghavan, K., Seigneur, C., 2005. Evaluation of three probing techniques in a three-dimensional air quality model. Journal of Geophysical Research 110, D02305. doi:10.1029/2004JD005248.

Zhang, Y., Hu, X.-M., Leung, L.R., Gustafson Jr., W.I., 2008. Impacts of regional climate changes on biogenic emissions and air quality. Journal of Geophysical Research 113, D18310. doi:10.1029/2008JD009965.